

Manuscript Number:

Title: Size-related mineralogical and surface physicochemical properties of the mineral particles from the recent sediments of the eastern Adriatic Sea

Article Type: Research paper

Section/Category: Environmental Chemistry (including Persistent Organic Pollutants and Dioxins)

Keywords: surface properties; submicron-sized mineral particles; organic matter; marine sediments; eastern Adriatic Sea

Corresponding Author: Professor Ivan Sondi,

Corresponding Author's Institution: Faculty of Mining, geology and petroleum Engineering, University of Zagreb

First Author: Maja Ivanić

Order of Authors: Maja Ivanić; Goran Durn; Srečo D Škapin; Ivan Sondi

Abstract: Mineral composition and surface physicochemical properties, i.e., specific surface area (SSA), cation exchange capacity (CEC), and surface charge (ζ -potential) of recent sediments and their submicron-sized mineral fractions from different sedimentological environments of the eastern Adriatic were investigated. The impact of organic matter on these properties was also examined. It was shown that illite and mixed-layered clay minerals (MLCM) were omnipresent and showed no size-related preferences while the occurrence of smectites, chlorites, and kaolinites varied. The content of smectites increased and of chlorites slightly decreased with particle size lowering. Sediments from the carbonate-rich environments did not contain smectites and chlorites and showed the highest content of kaolinite. For the first time, the poorly- and the well-crystallized kaolinite (K1 and K1D) were distinguished in the recent sediments of the Adriatic. While K1 prevailed in the submicron-sized fraction, K1D occurred only in micron-sized fractions. Authigenic submicron-sized aragonite was determined in a distinct environment of the semi-enclosed marine lake. The differences in mineral composition and particle size of sediments and their separated fractions were reflected in a wide range of the obtained SSA and CEC values. The highest values of SSA and CEC were determined in the submicron-sized fractions rich in phyllosilicates, 109 m²g⁻¹ and 87.4 cmol⁺kg⁻¹, respectively. The submicron-sized fraction from aragonite-rich marine lake showed the lowest values of SSA (56.4 m²g⁻¹) and CEC (38.8 cmol⁺kg⁻¹), still unexpectedly high for carbonate-rich environments. The removal of organic matter resulted in a significant increase in SSA and CEC, up to 150% and 76%, respectively.

Suggested Reviewers: Franz Ottner

Institut für Angewandte Geologie (IAG), Universität für Bodenkultur Wien, Austria

franz.ottner@boku.ac.at
He is an expert for clay mineralogy.

Frederico Spagnoly
Consiglio Nazionale delle Ricerche (CNR),, Istituto di Scienze Marine,
Italy
f.spagnoli@ismar.cnr.it
He has expertise in sedimentology and marine geology

Mladen Juračić
Department of Natural Science, Croatian Academy of Science and Arts,
Croatia
mjuracic@geol.pmf.hr
Expert in sedimentation processes of recent sediments

Sonja Lojen
Department of Environmental Science, Jožef Stefan Institute, Ljubljana,
Slovenia
sonja.lojen@ijs.si
Expert in geochemistry and carbonate sedimentology

Matej Dolenc
Faculty of Natural Sciences and Engineering, Department of Geology,
University of Ljubljana, Slovenia
matej.dolenc@geo.ntf.uni-lj.si
Expert in mineralogy and geochemistry

Jadran Faganeli
National Institute of Biology, National Institute of Biology, Piran,
Slovenia
jadran.faganeli@nib.si
Expert in biochemical processes in aquatic environment

Chemosphere
Editorial Office

January 21, 2020

To the Editorial Office:

Enclosed is the of the manuscript titled “**Size-related mineralogical and surface physicochemical properties of the mineral particles from the recent sediments of the eastern Adriatic Sea**” co-authored by Maja Ivanić, Goran Durn, Srečo D. Škapin, and Ivan Sondi, which we are submitting for the publication in the Chemosphere. Highlights and Graphical Abstract are included in the text of the manuscript.

Type of the Manuscript: Original scientific paper.

Statement:

The above manuscript and its contents have not been published previously. It is neither under consideration for publication in any other journal.

We appreciate your consideration,

Prof. Ivan Sondi

Highlights

- Micron and submicron-sized fractions of recent Adriatic sediments were investigated.
- Mineralogical and surface properties of mineral particles are size related.
- Phyllosilicate-rich submicron-sized sediment fraction showed highest SSA and CEC.
- The removal of organic matter resulted in a significant increase in SSA and CEC.
- Prevalence of submicron-sized authigenic aragonite induced low SSA and CEC.

Size-related mineralogical and surface physicochemical properties of the mineral particles from the recent sediments of the eastern Adriatic Sea

Ivanić, Maja¹, Durn, Goran², Škapin, Srečo D.³, Sondi, Ivan^{2*}

¹Ruđer Bošković Institute, Division for Marine and Environmental Research, Bijenička 54, 10000 Zagreb, Croatia

²Faculty of Mining, Geology and Petroleum Engineering, University of Zagreb, Pierottijeva 6, 10000 Zagreb, Croatia

³Department of Advanced Materials, Jožef Stefan Institute, Jamova cesta 39, 1000 Ljubljana, Slovenia

* Corresponding author: Ivan Sondi, email: ivan.sondi@rgn.hr

1 **Abstract**

2 Mineral composition and surface physicochemical properties, i.e., specific surface
3 area (SSA), cation exchange capacity (CEC), and surface charge (ζ -potential) of
4 recent sediments and their submicron-sized mineral fractions from different
5 sedimentological environments of the eastern Adriatic were investigated. The impact
6 of organic matter on these properties was also examined. It was shown that illite and
7 mixed-layered clay minerals (MLCM) were omnipresent and showed no size-related
8 preferences while the occurrence of smectites, chlorites, and kaolinites varied. The
9 content of smectites increased and of chlorites slightly decreased with particle size
10 lowering. Sediments from the carbonate-rich environments did not contain smectites
11 and chlorites and showed the highest content of kaolinite. For the first time, the
12 poorly- and the well-crystallized kaolinite (KI and KI_D) were distinguished in the recent
13 sediments of the Adriatic. While KI prevailed in the submicron-sized fraction, KI_D
14 occurred only in micron-sized fractions. Authigenic submicron-sized aragonite was
15 determined in a distinct environment of the semi-enclosed marine lake. The
16 differences in mineral composition and particle size of sediments and their separated
17 fractions were reflected in a wide range of the obtained SSA and CEC values. The
18 highest values of SSA and CEC were determined in the submicron-sized fractions
19 rich in phyllosilicates, 109 m²g⁻¹ and 87.4 cmol₊kg⁻¹, respectively. The submicron-
20 sized fraction from aragonite-rich marine lake showed the lowest values of SSA (56.4
21 m²g⁻¹) and CEC (38.8 cmol₊kg⁻¹), still unexpectedly high for carbonate-rich
22 environments. The removal of organic matter resulted in a significant increase in SSA
23 and CEC, up to 150% and 76%, respectively.

24 **Keywords:** surface properties, submicron-sized mineral particles, organic matter,
25 marine sediments, eastern Adriatic Sea.

26 **1. Introduction**

27 Mineral particles, the main component of sediments, play a major role in
28 biogeochemical processes in aquatic environment by controlling the fate and the
29 behaviour of organic and inorganic compounds through complex physicochemical
30 processes associated with their surfaces (Breiner et al., 2006; Hochella et al., 2008;
31 Plathe et al., 2013). During the last decade, numerous studies have shown that the
32 submicron-sized mineral particles, and particularly nanomineral solids, represent the
33 most reactive mineral phases in the environment, comprising over 90% of potentially
34 reactive surfaces (Breiner et al., 2006; Hochella et al., 2008; Plathe et al., 2013;
35 Sondi et al., 2017; Tang et al., 2009).

36 The micron- and the submicron-sized mineral fractions in sediments mostly consist of
37 clay minerals, metal oxides, and oxyhydroxides and sulphides (Perret et al., 1994;
38 Tang et al., 2009). It is generally accepted that carbonates occur as lithogenic and
39 biogenic micron-sized constituents in recent sediments, and can rarely be found in
40 the submicron-size fractions (Buffle et al., 1998; Perret et al., 1994), especially in the
41 nanosized dimensions (Wilkinson and Reinhardt, 2005). However, investigations of
42 carbonate minerals on the nanoscale are scarce and mostly focused on those of
43 biogenic origin (Morse et al., 2007).

44 The surface reactivity of mineral particles, which results from their structural,
45 chemical and surface properties, can be described by the specific surface area
46 (SSA), the cation exchange capacity (CEC) and the surface charge (ζ -potential).
47 These properties are used to describe physicochemical reactions occurring at the

48 surfaces of mineral particles (Bišćan et al., 1991; Breiner et al., 2006; Zhuang and
49 Yu, 2002) and are considered of great importance in different biogeochemical
50 processes.

51 Mineral particles in sediments are associated with various inorganic and organic
52 compounds that form micro- and macro-aggregates. It is assumed that more than
53 90% of organic matter (OM) is associated with the surfaces of mineral particles
54 (Hedges and Keil, 1995; Keil et al., 1994; Mayer, 1999). These organo-mineral
55 aggregates alter the physicochemical properties of mineral surfaces and contribute to
56 the preservation of OM (Kaiser and Guggenberger, 2003; Mikutta et al., 2005b;
57 Ransom et al., 1998).

58 Investigation of the surface physicochemical properties of the micron- and
59 submicron-sized mineral particles that are an integral part of the complex organo-
60 mineral aggregates occurring in natural environments requires their separation from
61 organic components (Citeau et al., 2006; Tang et al., 2009). The main endeavor
62 during this process is minimizing the alterations of mineral surfaces caused by
63 various physical and chemical treatments (Buffle and Leppard, 1995; Citeau et al.,
64 2006).

65 Previous studies carried out in the Adriatic region have provided information on the
66 primary sedimentological and mineralogical properties of recent sediments (Boldrin et
67 al., 1992; Faganeli et al., 1994; Matijević et al., 2008; Pigorini, 1968; Pikelj et al.,
68 2016; Ravaioli et al., 2003; Sondi and Juračić, 2010; Spagnoli et al., 2014; Tomadin,
69 2000a), their surface physicochemical properties (Bišćan et al., 1991; Boldrin et al.,
70 1992; Vdović et al., 1991) and their geochemical features (De Lazzari et al., 2004;
71 Dolenc et al., 1998; Goudeau et al., 2013; Spagnoli et al., 2014).

72 Still, the impacts of different mineral phases, particle size, and OM on the surface
73 physicochemical properties of recent sediments were not systematically investigated.
74 For the first time, this study aims to investigate the size-related mineralogical and
75 surface physicochemical properties of the mineral particles separated from recent
76 sediments from different sedimentological environments of the eastern Adriatic (an
77 estuary, a delta, deep-water open-sea areas, a marine lake, an indented marine bay).
78 Particular attention was given to the investigation of the submicron-sized fraction. In
79 addition, the impact of the OM on the surface physicochemical properties on these
80 solids was examined.

81 **2. Experimental**

82 **2.1. Study area**

83 The sampling locations (S1-S8) were distributed along the eastern coast of the
84 Adriatic Sea, as shown in Figure 1.

85

86 **Figure 1.**

87

88 The investigated sedimentological environments include coastal areas under a
89 significant riverine influence (S1, S2, and S5), deep-water open-sea areas (S3, S4,
90 and S8), a semi-enclosed karstic marine lake (S6) and an indented marine bay (S7).
91 Sampling station S1 is in the northern Adriatic, in the outer region of the area
92 receiving the Po River sediment load (Faganeli et al., 1994; Pigorini, 1968). Location
93 S2 is in the karstic Krka River estuary, below the calc tufa barriers formed at the
94 uppermost part of the estuary. The open-sea sampling stations S3 and S4 are

95 located at the central and the outer part of the Jabuka Pit depression, respectively.
96 Location S5 is in the Neretva Channel, in front of the Neretva River mouth, where the
97 river discharges its sediment load and forms a delta. The karstic marine lake (Malo
98 Jezero) on the island of Mljet (S6) represents a unique sedimentological system due
99 to the occurrence of intense short-term authigenic aragonite precipitation (Sondi and
100 Juračić, 2010; Sondi et al., 2017). The indented Risan Bay (S7) is the innermost part
101 of the Bay of Kotor, where hydrodynamic conditions allow deposition of fine-grained
102 material (Bellafiore et al., 2011; Pikelj and Juračić, 2013). Location S8 is in the
103 Albanian coastal area, under influence of the Drin River, the largest river on the
104 eastern Adriatic coast.

105 **2.2. Sampling and sample preparation**

106 Surface sediments (Fig. 1) were collected using a gravity corer (Uwitec, Austria).
107 Immediately after sampling, sediments were frozen and stored at -20°C. Before the
108 laboratory analyses, sediments were freeze-dried (FreeZone 2.5, Labconco, USA).

109 The sediment samples were treated as follows:

110 i. Native sediments

111 Fractionation was performed on samples representing distinct environments of
112 the northern (S1), central (S3) and southern (S6, S7) Adriatic. Sediments were
113 rinsed in deionized water to remove salts and increase particle dispersion.

114 ii. NaOCl-treated sediments

115 Fractionation was performed on all samples after OM was removed.

116 *2.2.1. The organic matter (OM) removal*

117 The OM was removed by the slightly modified treatment proposed by Kaiser and
118 Guggenberger (2003). Sodium hypochlorite (NaOCl) was chosen due to its effective
119 removal of the OM from carbonate-rich sediments at room temperature (Gaffey and
120 Bronniman, 1993; Mikutta et al., 2005a). Samples were dispersed in deionized water
121 and the pH of the dispersion was adjusted to 8.5 and constantly controlled during the
122 treatment. After the NaOCl-treatment, sediments were sequentially rinsed with
123 deionized water by centrifugation. After rinsing, samples were thoroughly stirred with
124 deionized water in a beaker and left to settle in order to perform the particle size
125 fractionation.

126 *2.2.2. Particle size fractionation*

127 Size fractions (<8 μm , <4 μm , <2 μm , <1 μm and <0.45 μm) were collected from the
128 NaOCl-treated sediment samples and several native sediments (S1, S3, S6, and S7).
129 Different fractions were obtained from aqueous dispersions at 25°C by gravitational
130 settling, a low-invasive fractionation technique that enabled separation of a sufficient
131 amount of material. Fractionation was performed according to the periods presented
132 in Table S1 (Supplementary). To determine if the particle falls into the desired size-
133 range, the collected suspensions were analysed by dynamic light scattering (LS
134 13320 Beckman Coulter Inc., USA). Example of the particle size distribution (PSD)
135 curves of the collected fractions is shown in Figure S1 (Supplementary). Only
136 samples containing a minimum of 97 vol.% of particles of the required size were
137 freeze-dried and used for further analysis.

138 It was demonstrated that the time required for the separation of mineral particles of
139 the desired size significantly differed from the calculated values that are based on the
140 Stokes' law (Table S1, Supplementary). Clifton et al. (1999) investigated the

141 efficiency of the size fractionation after Stokes' law and found that, even though the
142 mean size (Mz) of particles was in the desired size-range, the number of misplaced
143 particles ranged from 25-65%. The reasons for this discrepancy can be found in the
144 Brownian motion of the submicron-sized particles and assumptions that all particles
145 are spherical and of the same density, as Stokes' law anticipates. Obviously, this
146 assumption cannot be applied to natural sediment samples.

147 **2.3. Analytical methods**

148 *2.3.1. Sediment characterization*

149 Particle-size distribution (PSD) measurements were performed by laser diffraction
150 (LS 13320, Beckman Coulter Inc., USA). Prior to measurements, samples were
151 dispersed in deionized water and treated with ultrasound for 3 minutes. The particle
152 size was calculated with proprietary software using the Mie theory of light scattering
153 (optical parameters: refractive index 1.53; absorption index 0.1). Sediments were
154 classified according to Shepard's classification scheme (1954) and the modified
155 Wentworth (1922) grade scale with the clay-silt boundary at 2 μm .

156 *2.3.2. Mineralogical analysis*

157 The total carbonate content was determined volumetrically with the Scheibler's
158 apparatus (Allison and Moodie, 1965). Particle size and morphology were examined
159 by the high-resolution scanning field-emission electron microscopy (HR-FE-SEM,
160 Zeiss Supra 35 VP, Germany). The mineral composition of native sediments was
161 determined by the X-ray powder diffraction (XRD) using a D4 Endeavor
162 diffractometer (Bruker AXS, Germany). The mineral composition of fractions smaller
163 than 2 μm , 1 μm and 0.45 μm (where available) was determined using a Philips

164 diffractometer (graphite monochromator, Cu-K α radiation, proportional counter). The
165 XRD patterns of random samples were obtained after air-drying. The XRD patterns of
166 oriented samples were obtained after the following treatments: (a) K-saturation, (b) K-
167 saturation and DMSO solvation, (c) K-saturation and ethylene glycol solvation, (d) K-
168 saturation and heating for two hours at 350°C, (e) K-saturation and heating for two
169 hours at 550°C, (f) Mg-saturation, (g) Mg-saturation and ethylene glycol solvation, (h)
170 Mg-saturation and heating for two hours at 350°C and (i) Mg-saturation and heating
171 for two hours at 550°C. The non-clay mineral phases were identified using the
172 Powder Diffraction File (1996) data system and the Panalytical XPert HighScore (v.
173 1.0d) program package. Identification of clay minerals was generally based on the
174 methods outlined by Brindley and Brown (1980), and Moore and Reynolds (1989).
175 The term “MLCM” was used for mixed-layer clay mineral(s), in which the type of
176 interstratification and the constituting clay minerals were not recognized with
177 certainty. The DMSO-treatment enabled the differentiation of the poorly-crystallized
178 kaolinite that does not intercalate with DMSO (KI), from the well-crystallized kaolinite
179 that forms intercalation compounds with DMSO (KI_D) (Range et al., 1969). The
180 semiquantitative estimates of clay minerals in the <2 μm , <1 μm and <0.45 μm
181 fractions were based on the relative intensities of the characteristic X-ray peaks.
182 Estimated quantities of minerals were presented with Xs, but no quantitative value
183 was assigned to each X.

184 *2.3.3. Determination of the total carbon, the total organic carbon (TOC) and the total* 185 *inorganic carbon (TIC) content*

186 The total carbon and the total organic carbon (TOC) were determined in a Leco IR–
187 212 (USA) carbon analyser. The TOC, which is used as an indicator of the OM

188 content, was determined by combustion of acid insoluble matter, after treatment with
189 hot 1:1 diluted 36.5% HCl. The content of TIC was calculated from the difference
190 between the total carbon and TOC.

191 *2.3.4. The surface physicochemical characterization*

192 The specific surface area (SSA) measurements were performed by a single-point
193 nitrogen adsorption using the BET method, on a FlowSorb II 2300 instrument
194 (Micromeritics, USA). The cation exchange capacity (CEC) was determined using an
195 ammonia selective electrode based on the method described by Busenberg and
196 Clemency (1973). The electrophoretic mobility (EPM) was measured using a
197 Zetasizer Nano ZS (Malvern, UK). For the measurements, 10 mg of sediment sample
198 was dispersed in 50 ml of an inert electrolyte (1 mM NaCl) and left for a few hours to
199 reach equilibrium. The electrophoretic mobility was measured at a constant
200 temperature of 25°C. The software automatically calculated the ζ -potential from the
201 EPM using Henry's equation (Hunter, 1981). The instrument was calibrated prior to
202 measurements with a polystyrene latex standard, supplied by the manufacturer. All
203 the data processing was evaluated using Zetasizer software 6.20 (Malvern, UK).

204

205 **3. Results and discussion**

206 **3.1. Granulometric characteristics of the investigated sediments**

207 The native sediments were classified as silty sand (S1), silt (S5-S8), and clayey silt
208 (S2-S4) (Fig. S2a, Supplementary).

209 Coarser sediments were found in the northern Adriatic (S1), the Neretva Channel
210 (S5), and the Albanian coastal area (S8). These environments coincide with areas

211 where rivers with a large discharge such as Po, Neretva, and Drin, deposit their load
212 in marine coastal environments. The prevalence of silts was also characteristic for
213 the carbonate-rich sediments at the Krka River estuary (S2) and Malo Jezero on the
214 island of Mljet (S6), and for the Risan Bay (S7) where surface freshwater run-off
215 significantly contributes to the size and the mineral composition of the sediment.
216 Fine-grained sediments were found in the central Adriatic open-sea area (S3, S4),
217 where due to specific hydrodynamic conditions of the Adriatic basin and the limited
218 coastal influence, deposition of finer particulate material occurs. The obtained results
219 are in agreement with the previous research that showed deposition of finer sediment
220 in the central Adriatic area and coarser sediments in the northern part of the Adriatic
221 and along its eastern coast (De Lazzari et al., 2004; Spagnoli et al., 2014; Tomadin,
222 2000a; Vdović and Juračić, 1993).

223 Following the OM removal (Fig. S2b), all sediments were classified as clayey silts.
224 This is the result of an increase in the share of clayey content and a decrease in
225 particle size. Since most of the OM is found in organo-mineral aggregates (Arnarson
226 and Keil, 2007), its removal caused their disintegration and the subsequent release
227 of finer particles.

228 When comparing corresponding size fractions separated from the native and the
229 NaOCl-treated sediment samples (Table S1, Supplementary), it was observed that
230 the native sediment fractions $<8 \mu\text{m}$ and $<4 \mu\text{m}$ contained slightly coarser material
231 and a correspondingly higher Mz. However, the Mz of fine fractions ($<2 \mu\text{m}$, $<1 \mu\text{m}$,
232 $<0.45 \mu\text{m}$) from both sets of samples was in the same size range. This implies that
233 the removal of OM induced disintegration of macro-aggregates and had little effect on
234 the OM bound to the clayey mineral particles.

235 Indeed, the results displayed in Figure 2a show an increase in the amount of TOC
236 with decreasing particle size (sampling station S3). The strong affinity of the OM for
237 finer particles was already established (Bišćan et al., 1991; Buffle and Leppard,
238 1995). This results in their strong association and greater resistance to chemical
239 treatments (Kahle et al., 2003; Mikutta et al., 2005b).

240 Indeed, Keil et al. (1994) have shown that diverse classes of OM were associated
241 with different types of mineral particles. Namely, coarser particles were enriched in
242 carbon-rich OM while smaller, particularly clayey particles, contained nitrogen-rich
243 OM. These diversities may lead to differences in the degradation rate of OM
244 associated with the surfaces of mineral particles.

245 Finally, the persistence of clayey particles in the water column, together with their
246 prolonged oxygen exposure time (Coppola et al., 2007), could lead to the removal of
247 the more labile organic compounds, leaving the residual OM tightly bound to mineral
248 surfaces and contributing to its resistance to the applied chemical treatment.

249

250 **Figure 2.**

251

252 It is noteworthy that after the OM removal, similar PSD curves were obtained for the
253 corresponding size-fractions in all investigated sediments (Fig. 3). A general lowering
254 in modality, i.e. number of frequency peaks, with a decrease in the particle size
255 occurred. Minor discrepancies were observed only for the carbonate-rich sediment
256 from Malo Jezero (S6). In addition, the mineralogical analysis revealed presence of,
257 in general, similar mineral phases in the corresponding size fractions of the

258 investigated sediments, as shown in section 3.2. A similar conclusion was reached by
259 Keil et al. (1994) when exploring size fractions of sediments along the Washington
260 margin (USA). Comparable granulometric characteristics of the corresponding size
261 fractions could result from prevalence of similar mineral phases. The observed shift in
262 the PSD curves of size fractions from the Malo Jezero (S6) sediment, characterized
263 by slightly different mineral composition, supports this assumption. However,
264 considering the strong affinity between OM and mineral surfaces, and its incomplete
265 removal from the investigated samples (Table 1), it seems reasonable to presume
266 that OM, through formation of aggregates, contributed to the observed similarity in
267 PSD. Its influence was probably most exerted in fine fractions, due to its increased
268 content in this size range (Fig. 2a).

269 A unimodal PSD curve with a small tail at 0.25 μm and a Mz of 0.1 μm was
270 characteristic for all investigated fractions $<0.45 \mu\text{m}$ (Fig. 3). Despite prolonged
271 settling time, appreciable share of particles in smaller size range was not attainable.
272 Plathe et al. (2013) suggested that in aquatic environments, nanoparticles in the size
273 of 5-20 nm are mostly found in aggregates of ~ 100 nm, and the efficiency of
274 aggregate disintegration is limited. The obtained Mz of 0.1 μm , observed in the finest
275 fractions (Table S1, Supplementary), supports this assumption. According to
276 Baalousha (2009), disintegration of micron-sized aggregates produces smaller
277 aggregates that are 50 to 400 nm in size, which can be further disintegrated by a
278 much slower process of surface erosion. Rapid aggregation of the nanosized
279 particles and their limited disintegration could be a valid explanation for the observed
280 difficulties in extracting them from the dispersion considering the settling time.

281

282 **Figure 3.**

283

284 **3.2. Mineralogical characteristics of the investigated sediments**

285 3.2.1. Carbonate mineral phases

286 The share of carbonates in native sediments varied from 14% to 69% (Table 1).
287 Calcite, Mg-calcite, aragonite, and dolomite were determined as major or minor
288 constituents (Table 1). According to their carbonate content, the investigated
289 sediments can be divided into two groups. The first group, including sediments at
290 sampling stations S1-S6, is characterised by a significant carbonate content (>27%),
291 originating from weathering of the karstic rocks in the drainage area of the eastern
292 Adriatic coast, the appearance of biomineral fragments, and the authigenic formation
293 of carbonate minerals in the marine environment. Sediments at sampling stations S7
294 and S8, which contain significantly lower share of carbonates, ~15%, and calcite as
295 the only carbonate mineral phase (Table 1), belong to the second group. Among the
296 first group, sediments from the Krka River estuary (S2) and Malo Jezero (S6)
297 contained the highest amounts of carbonates, 59% and 69%, respectively (Table 1).
298 However, the origin and the mineral composition of carbonates in these two systems
299 were different. In the Krka River sediment (S2) calcite was the only determined
300 carbonate mineral phase (Table 1, Fig. 4f). Previous investigations of these
301 sediments indicate its detrital origin with a small contribution of biogenic components
302 (Juračić and Prohić, 1991). Contrarily, the XRD analysis of native sediment from
303 Malo Jezero (S6) showed the presence of aragonite, Mg-calcite, and calcite (Table
304 1). Aragonite was the most abundant mineral phase. Sondi and Juračić (2010) have
305 shown that biologically induced precipitation of aragonite, occurring during the short-

306 term whitening events, mainly contributed to the high share of carbonates,
307 particularly aragonite in recent sediment of Malo Jezero (S6). The FE-SEM
308 photomicrographs (Fig. 4d) revealed the prevalence of irregular needle-like mineral
309 particles, typical for the occurrence of authigenic aragonite in the marine environment
310 (Sondi and Juračić, 2010). In the fine fractions from these two sediments (Fig. 4 d,f),
311 only occasional appearance of calcite grains was observed in sampling station S2,
312 while irregular aragonite particles were abundant even in the submicrometer size-
313 range (S6). The occurrence of aragonite and Mg-calcite in recent sediments of the
314 Adriatic was mainly associated with biogenic production (Pikelj et al., 2016). Indeed,
315 Mg-calcite was determined in the central Adriatic open-sea sediments (S3 and S4)
316 (Table 1), where the abundance of skeletal detritus (Fig. 4e), indicates its biogenous
317 origin. According to previous investigations, carbonates in the Adriatic sediments are
318 found mainly in the coarse-grained fractions (Faganeli et al., 1994; Pikelj et al.,
319 2016). A decrease in their share with decreasing particle size in majority of samples,
320 and the absence of Mg-calcite in finer fractions from the open-sea sediment (S3)
321 (Tables 1, 2), supports these assumptions.

322

323 **Figure 4.**

324

325 However, the XRD and FE-SEM investigation of different size fractions separated
326 from the carbonate-rich sediment from Malo Jezero (S6) showed a considerable
327 share of aragonite present in the submicron-sized fraction (Table 2, Fig. 4d). This
328 finding is not in line with the general assumption that carbonate particles do not occur
329 in the finest sediment fractions, especially in the nanosized dimensions (Buffle et al.,

330 1998; Wilkinson and Reinhardt, 2005). Their presence in sediment from Malo Jezero
331 (S6) is a rare example of appearance of nanosized carbonates in recent sediments
332 that highlights the important role of authigenic processes in their formation.

333 The lower share of calcite in sediments at sampling stations S7 and S8 (Table 1) is in
334 agreement with the observation reported by Faganeli et al. (1994). These stations are
335 located in the coastal areas of Montenegro and Albania where lithology of the
336 hinterland mostly consists of flysch deposits, metamorphic, and igneous rocks
337 (Dolenec et al., 1998; Pikelj and Juračić, 2013; Rivaro et al., 2004). The material
338 formed by weathering of these terrains is transported by the Albanian rivers and is
339 the main source of sediment deposited in the coastal area.

340 Dolomite was determined in sediments from the northern Adriatic (S1) and the
341 Neretva Channel (S5). According to previous investigations, detrital dolomite in
342 northern Adriatic originates from the drainage area of the eastern Alps (Faganeli et
343 al., 1994; Pikelj et al., 2016; Ravaioli et al., 2003). Dolomite at sampling station S1
344 could also originate from the Late Glacial loess deposits. Namely, Durn et al. (2018a)
345 found dolomite in the Late Glacial loess on the island of Susak (Northern Adriatic).
346 The possible source of dolomite in the Neretva Channel (S5), where it was found
347 even in the submicron-size fraction (Table 2), are flysch sediments. Particulate
348 material entering the sedimentation system mostly originates from weathering of the
349 Eocene flysch deposits in the upper drainage area (Jurina et al., 2015), in which
350 dolomite is a common component in the Adriatic zone (Pikelj et al., 2016; Toševski et
351 al., 2012).

352 3.2.2. Clay minerals

353 The XRD investigation of clay minerals in the investigated sediments showed
354 presence of illite, smectite, chlorite, kaolinite, I/S MLCM and MLCM (Table 2).
355 Although these results are generally in agreement with the earlier investigations
356 (Ilijanić et al., 2014; Tomadin, 2000a), the new data were acquired based on the
357 analysis of different micron- and submicron-sized sediment fractions of the Adriatic
358 sediments, and provides a more detailed identification of clay minerals.

359 Illite was the most abundant and omnipresent clay mineral in the investigated
360 sediments and equally present in all size fractions (Table 2). Mixed-layer clay
361 minerals (MLCM and/or I/S MLCM) were also found in all investigated sediments and
362 generally showed no size-related preferences (Table 2). Smectites were most
363 abundant in sediments from the open-sea areas, and in general, their content
364 increased with particle size lowering (Table 2). Chlorites occurred together with
365 smectites, however their share mostly decreased in finer size fractions.

366 In the central Adriatic area, low hydrodynamic conditions allow deposition of very fine
367 particulates (Spagnoli et al., 2014). The material deposited in this area consists of the
368 clayey fraction delivered by currents flowing southward from the northern Adriatic,
369 northwest from the southern Adriatic and the material of aeolian origin (Dolenec et
370 al., 1998; Faganeli et al., 1994; Goudeau et al., 2013; Tomadin, 2000a). According to
371 Tomadin (2000a), this area is supplied by the off-shore Padane flux, carrying fine-
372 grained material rich in illite and chlorite which is delivered by the Po River, and with
373 seasonal input of the coastal Apennine flux, transporting materials of Apennine
374 source that are rich in smectites.

375 In the carbonate-rich sediments of the Krka River estuary (S2) and Malo Jezero (S6),
376 smectites and chlorites were not determined (Table 2). These clay minerals mainly

377 originate from the flysch deposits located in the drainage area of the Adriatic.
378 However, sampling stations S2 and S6 are surrounded by carbonates with no flysch
379 terrains that could directly act as a source of smectites and chlorites. Due its distance
380 from the coast, terrigenous supply in Malo Jezero (S6) is limited to soil erosion and
381 aeolian deposition while its enclosure limits the water exchange, restricting potential
382 input of material by currents. The small amount of the suspended load carried by the
383 Krka River is retained by the calc tufa barriers located upstream from the sampling
384 station S2. The main source of the flysch material deposited in the Krka River estuary
385 is located downstream of the sampling station (Juračić and Prohić, 1991).

386 Kaolinites were found in sediments of the northern and the central Adriatic area (S1-
387 S6), but they were not determined with certainty in sediments of the coastal areas of
388 Montenegro and Albania (S7 and S8, respectively). Moreover, the results of this
389 study for the first time allowed differentiation between the well-crystallised kaolinite
390 (KI_D) and the poorly-crystallised kaolinite (KI) in the investigated sediments. Results
391 in Table 2 revealed that the KI_D was not present in the submicron-sized fractions,
392 while the KI was equally abundant in the submicron and the clayey fractions.
393 Rodriguez-Navarro et al. (2018) observed similar size-fractionation of kaolinite in the
394 Saharan dust particles deposited in the Iberian Peninsula and ascribed it to different
395 sources of dust. Coarser kaolinite particles of higher crystallinity were present in the
396 silt fraction and the finer particles of poor crystallinity in the clay fraction. According to
397 Tomadin (2000b), kaolinite in the Adriatic sediment is of both river-borne and aeolian
398 origin. The wind-blown dust from different source areas in Africa has a significant
399 effect on sediments in the Adriatic. However, since the contribution from the wind-
400 blown transport in sediments is usually masked by the more significant river supply
401 (Tomadin, 2000b), their presence can be revealed in sediments where the input of

402 terrigenous siliciclastic material is limited. Indeed, the two sediments from the
403 carbonate-rich environments, Krka River estuary (S2) and Malo Jezero (S6), showed
404 the highest content of the KI. It can therefore be argued, that the KI in the Adriatic
405 sediments is of both river-born and aeolian origin, as Tomadin (2000b) postulated.
406 However, kaolinite was determined in polygenetic soil, different palaeosols and loess
407 sediments on the island of Susak (Durn et al., 2018a, b). Durn et al. (1999)
408 postulated that kaolinite in the fine clay (KI) of the Istrian Terra Rossas is
409 predominantly authigenic (pedogenic), while the KI_D is considered inherited from the
410 parent materials. Durn et al. (2019) found that kaolinites (both KI and KI_D) and illitic
411 material are the dominant clay mineral phases in the analysed Terra Rossa and
412 Calcocambisol from Istria.

413 It is important to note that the clay mineral assemblage at sampling station S1 (illite,
414 chlorite, smectite, kaolinites and I/S MLCM) is identical to that found in the Late
415 Glacial loess deposits on the island of Susak (Durn et al., 2018a). This points to the
416 same provenance of the material from which the Late Glacial loess on the island of
417 Susak and sediments at sampling station S1 were derived. Generally, clay minerals
418 in the Adriatic sediments originate from the material delivered by the Po River and
419 rivers draining the Apennines, from the Albanian rivers on the southeast part of the
420 Adriatic and aeolian transport of Saharan dust (Tomadin, 2000a). However, during
421 the Pleistocene, the North Adriatic was a closed basin and the sea level was up to
422 100 m lower than today. Fluvial material was exposed to wind activity during the
423 glacials and was subsequently deposited to form loess and aeolian sand. During the
424 interglacials and interstadials, aeolian sedimentation was interrupted by the soil
425 forming processes. Therefore, loess, aeolian sand, soils, and palaeosols have to be
426 considered as a potential source of clay minerals in the recent Adriatic sediments

427 (e.g. Durn and Frechen, 2018c), in addition to flysch deposits, as documented by the
428 clay mineral composition (e.g. smectite, chlorite, illite) of sediment in the Neretva
429 Channel (S5).

430 3.2.3. Other mineral phases

431 Plagioclases were found in the recent sediment of the open-sea environment (S3), in
432 sediments of the Neretva Channel (S5) and the Risan Bay (S7), while both
433 plagioclases and K-feldspars were determined in sediments of the northern Adriatic
434 (S1) and Malo Jezero (S6) (Table 1). The weathering of feldspars does not produce
435 submicron-sized particles (Table 1).

436 Pyrite was found in sediments from the Krka River estuary (S2), Malo Jezero (S6),
437 northern Adriatic (S1) and the Neretva Channel (S5) (Tables 1, 2). Formation of
438 pyrite is associated with reductive conditions in sediments, induced by increased
439 productivity and degradation of a large amount of OM of terrigenous origin in the
440 investigated areas (Giani et al., 2012; Jurina et al., 2015). In reducing conditions and
441 the presence of a sulfidic zone, pyrite can be formed during the post-depositional
442 early-diagenetic processes. Indeed, the framboidal structure of pyrite of several
443 microns in size, composed of uniform submicron-sized crystals (Fig. 4c) in sediment
444 at sampling station S6 confirms its diagenetic origin (Wilkin et al., 1996).

445

446 **Table 1.**

447 **Table 2.**

448

449

450 **3.3. Surface physicochemical properties of the investigated sediment samples**

451 The SSA and CEC values of the investigated native sediments varied significantly
452 according to the sampling sites and ranged from 11.3 to 27.8 m²g⁻¹, and from 11.6 to
453 35.3 cmol_ckg⁻¹, respectively (Table S2). The highest values were obtained for
454 sediments in the open-sea area (S3, S4), in the Albanian coastal area (S8), and the
455 Risan Bay (S7). These sediments were fine-grained and mostly consisted of clay
456 minerals (Table 2). The lowest values were determined in sediments under the
457 dominant influence of rivers (S1 and S5). These sediments were coarser and
458 consisted of sand and silt fractions (Fig. S2a). Similar values were also obtained for
459 the silty carbonate-rich sediments at sampling stations S2 and S6. This is related to
460 the significant occurrence of carbonate mineral phases, which exhibit low SSA and
461 CEC values. The obtained results exemplify the predominant influence of particle
462 size and mineral composition on the determined SSA and CEC values.

463 The ζ-potentials of native sediments, at pH of natural waters (7.4 – 9.5), were in a
464 narrow range of values, from -30.7 mV to -26 mV (Table S2, Supplementary). It
465 should be noted that the measurements were carried out on native samples
466 dispersed in 1mM NaCl solutions and that the pH of dispersions were not adjusted to
467 the same pH values. These results confirm previous findings on the crucial role of OM
468 in the formation of the surface charge on mineral particles in natural environments
469 (Breiner et al., 2006; Buffle et al., 1998; Plathe et al., 2013). Even a small amount of
470 OM attached to the surfaces of mineral particles provides them with similar surface
471 charges at pH values from 7 to 10 (Durn et al., 2019; Sondi et al., 1997). This is
472 accomplished through complex processes of electrostatic attraction and ligand
473 exchange between the hydroxyl groups on the mineral surfaces and carboxyl and

474 phenolic groups of the organic matter (Gu et al., 1994; Tombácz and Szekeres,
475 2004).

476 **3.3.1. Influence of OM on the surface physicochemical properties of the** 477 **investigated sediments**

478 The OM significantly affects physicochemical properties (SSA and CEC) of mineral
479 surfaces (Bišćan et al., 1991; Boldrin et al., 1992; Kleber et al., 2004; Ransom et al.,
480 1998; Zhuang and Yu, 2002). The extent of modification can be estimated through
481 changes of these properties following the OM removal from mineral surfaces.

482 The applied NaOCl-treatment removed 53% to 82% of the OM from the investigated
483 sediments (Table 1). After the OM removal, the SSA of sediments ranged from 25.1
484 to 52.4 m²g⁻¹, and CEC from 18.5 to 39.1 cmol_ckg⁻¹ (Table S2, Supplementary). The
485 significant increase in SSA (47-150%) and CEC (5-76%) corresponds to the
486 observed granulometric changes (Fig. S2, Supplementary), indicating disintegration
487 of organo-mineral aggregates after the OM removal and exposure of new mineral
488 surfaces. Numerous studies reported an increase of SSA after the OM removal
489 (Boldrin et al., 1992; Durn et al., 2019; Kahle et al., 2003; Kaiser and Guggenberger,
490 2003; Kleber et al., 2004). However, contrary results were also reported (Bišćan et
491 al., 1991; Jurina et al., 2015; Vdović and Juračić, 1993). The influence of OM on the
492 surface physicochemical properties of mineral particles is complex and depends on
493 the type of OM, marine vs. terrigenous (Bišćan et al., 1991), and the character of the
494 underlying clay mineral surfaces (Zhuang and Yu, 2002). According to Bišćan et al.
495 (1991), the impact of OM on the reactivity of mineral particles depends on the
496 molecular weight and the porosity of the OM. The riverine type of OM, characterized
497 by the degradable, hydrophilic organic compounds, and the more persistent

498 hydrophobic OM, which is characteristic for marine environments, exhibit complex
499 and diverse influence on SSA and CEC of mineral surfaces (Bišćan et al., 1991).
500 These interactions are additionally complicated by the observed size-dependent
501 distribution of different organic compounds. According to Kiel et al. (1998), the share
502 of amino acids increases in fine fractions, carbohydrates in silty fraction, while lignin
503 phenols prevail in sandy fraction. Previous research showed that OM forms patches
504 and occurs at specific localities on the surface of mineral particles (Mayer, 1999;
505 Mikutta et al., 2005b; Ransom et al., 1997). If a significant part of the mineral surface
506 remains exposed, it can be presumed that the role of the OM in lowering SSA and
507 CEC of mineral particles is mostly in gluing grains into aggregates.

508 In addition, the results showed that the OM removal induced a more significant
509 increase of SSA compared to CEC values (Table S2, Supplementary). If the binding
510 of OM occurs on the more reactive sites on mineral surfaces, this indicates that the
511 edge (amphoteric) surfaces of clay minerals would be mostly associated with OM
512 (Kahle et al., 2003; Kaiser et al., 2002; Kaiser and Guggenberger, 2003; Mikutta et
513 al., 2005b). This would leave the basal and the interlayer siloxane surfaces free to
514 exchange cations with the surroundings. However, the role of OM cannot be
515 neglected, and since its removal was incomplete (Table 1), the remaining OM could
516 contribute to the determined CEC of the NaOCl-treated samples.

517 The incomplete removal of OM is also considered the main reason for the observed
518 negligible effect of the NaOCl-treatment on the ζ -potential values (Table S2,
519 Supplementary). It was already established that the ζ -potential of clay mineral
520 surfaces was significantly influenced by a small amount of fulvic and polyacrylic acid

521 (Sondi et al., 1997). This supports the assumption that even small amounts of the
522 OM govern the formation of surface charge of mineral particles.

523 ***3.3.2. Size-related variations in the surface physicochemical properties of the*** 524 ***investigated sediments***

525 A significant increase of SSA and CEC values occurred in finer size fractions in all
526 investigated sediments (Fig. 5). The reason for this is the reduction in particle size
527 and, more importantly, the presence of minerals with higher surface reactivity, e.g.
528 clay minerals (illite, I/S MLCM, smectite, kaolinite, chlorite).

529 The significant impact of mineral composition on the increase of SSA and CEC
530 values can be observed from the comparison of the two carbonate-rich sediments
531 from the Krka River estuary (S2) and Malo Jezero (S6). While native sediments
532 exhibited similar SSA and CEC values (Table S2, Supplementary), significant
533 changes were observed with decreasing particle size (Fig. 5). In sediment at
534 sampling station S2, a rise in SSA and CEC values was observed already in the
535 fraction <8 µm, while further reduction in grain size caused an additional increase of
536 both parameters (Fig. 5). These results suggest that carbonate minerals,
537 characterized by low surface reactivity, were predominantly found in coarser
538 fractions, and efficiently removed by fractionation in the first step. The remaining clay
539 minerals in finer fractions (illite, poorly-crystallised kaolinite and I/S MLCM), caused a
540 more significant increase of SSA and CEC (Fig. 5). Contrarily, size fractions
541 separated from sampling station S6 exhibited a minor increase with particle size
542 lowering, and the lowest SSA and CEC values. The reason for this is the presence of
543 carbonates (calcite, Mg-calcite and aragonite) in all size fractions (Table 2, Fig. 4d), a
544 lower share of clay minerals (illite, kaolinite and MLCM) and the absence of I/S

545 MLCM (Table 2). This indicates a low surface reactivity of carbonates even when
546 they are present in submicron-sized dimensions.

547 The increase of SSA and CEC in the finest fractions ($<0.45\ \mu\text{m}$) was not observed as
548 expected. The reason for this can be found in the increase of the TOC content (Fig.
549 2a), suggesting strong association of OM to mineral surfaces in the submicron-sized
550 mineral phases (Kahle et al., 2003; Mikutta et al., 2005b). Mikutta et al. (2005b)
551 showed that more SSA was occupied by the OM in the size fraction $<0.2\ \mu\text{m}$
552 compared to coarser particles, e.g. $0.2 - 2\ \mu\text{m}$. In addition, it was shown that the
553 interaction of clay minerals and the OM depends on the different types of OM and
554 specific clay minerals (Ransom et al., 1998). In particular, Ransom et al. (1998)
555 showed that the preservation of OM was higher in sediments rich in smectites,
556 compared to chlorite-dominated sediments. Indeed, the results showed that samples
557 with increased share of smectites in the finest fraction (Table 2) exhibited a decrease
558 of SSA values. Complex interactions of specific clay minerals and OM could have,
559 therefore, contributed to the observed changes in SSA and CEC of the finest
560 fractions. A continuous size-dependent increase of both SSA and CEC determined in
561 sediment from Malo Jezero (S6) supports these assumptions. Sediment from this
562 location showed unique characteristics, with carbonates present in all size fractions
563 and a minor share of the non-expandable clay minerals determined in the submicron-
564 sized fraction (Table 2). The observed mineral composition could have contributed to
565 a more straightforward relationship between the mineral surfaces and OM, mostly
566 governed by weaker associations of carbonates and the OM. The presence of
567 different types of OM, e.g. non-degradable terrigenous plant debris from the
568 surrounding area (Lojen et al., 2010) and the plankton remains from intense primary

569 production during summer periods (Sondi and Juračić, 2010), could have induced the
570 occurrence of particulate OM, not associated with mineral surfaces.

571

572 **Figure 5.**

573

574 **Conclusion**

575 For the first time, the mineral composition and the surface physicochemical
576 properties of successive sediment size fractions from different sedimentological
577 environments of the eastern Adriatic were investigated. Special attention was given
578 to the submicron-sized sediment fractions and the influence of OM on the surface
579 reactivity of mineral particles. It was shown that the mineral composition and the
580 content of clay minerals were different in the studied environments and moderately
581 varied among the separated micron/submicron-sized fractions. Illite and MLCM were
582 omnipresent and showed no size-related preferences while the occurrence of
583 smectites, chlorites, and kaolinites varied. The content of smectites increased in the
584 submicron-size fraction, while the share of chlorite decreased with particle size
585 lowering. Sediments from the carbonate-rich environments did not contain smectite
586 and chlorite and showed the highest content of kaolinite. The poorly-crystallised
587 kaolinite prevailed in the submicron-sized fraction and the well-crystallised kaolinite
588 was limited to the micron fraction. Increase in the surface reactivity of mineral
589 particles with the particle size lowering was related to smaller particle size and
590 accumulation of minerals characterised by large SSA and CEC (e.g. clay minerals).
591 Authigenic formation of the nanosized carbonate minerals resulted in their increased

592 presence even in the submicron-size fraction, resulting in lower SSA and CEC
593 values. The OM removal induced disintegration of macroaggregates and exposure of
594 mineral surfaces, reflected in an increase of SSA and CEC values.

595 **Acknowledgments**

596 The authors appreciate the contribution of Kristina Pikelj for providing sediment
597 samples S1, S3 and S4 and Tamara Troškot-Čorbić for determination of the total
598 carbon and the TOC content.

599

600 **Supplementary information**

601 **Table S1.**

602 **Table S2.**

603 **Figure S1.**

604 **Figure S2.**

605 **References**

606 Allison, L.E., Moodie, C.D., 1965. Carbonate. In: Black, C.A. (Ed.), Methods of
607 Soil Analysis, Part 2, second ed., pp. 1379-1400 Agronomy Monography 9 ASA,
608 CSSA and SSSA.

609 Arnarson, T.S., Keil, R.G., 2007. Changes in organic matter–mineral interactions
610 for marine sediments with varying oxygen exposure times. *Geochim. Cosmochim.*
611 *Ac.* 71, 3545-3556.

612 Baalousha, M., 2009. Aggregation and disaggregation of iron oxide nanoparticles:
613 Influence of particle concentration, pH and natural organic matter. *Sci. Total*
614 *Environ.* 407, 2093-2101.

615 Bellafiore, D., Guarnieri, A., Grilli, F., Penna, P., Bortoluzzi, B., Giglio, F., Pinardi,
616 N., 2011. Study of the hydrodynamical processes in the Boka Kotorska Bay with
617 a finite element model. *Dynam. Atmos. Oceans* 52, 298-321.

618 Bišćan, J., Rhebergen, I., Juračić, M., Martin, J.M., Mouchel, J.M., 1991. Surface
619 properties of suspended solids in stratified estuaries (Krka River estuary and
620 Rhône River delta). *Mar. Chem.* 32, 235-252.

621 Boldrin A., Juračić, M., Menegazzo Vitturi, L., Rabitti, S., Rampazzo, G., 1992.
622 Sedimentation of riverborne material in a shallow shelf sea: Adige River, Adriatic
623 Sea. *Mar. Geol.* 103, 473-485.

624 Breiner, J.M., Anderson, M.A., Tom, H.W.K., Graham, R.C., 2006. Properties of
625 surface – modified colloidal particles. *Clay Clay Miner.* 54, 12-24.

626 Brindley, G.W., Brown, G., 1980. Crystal Structures of Clay Minerals and Their X-
627 ray Identification. Mineralogical Society, London, pp. 495.

628 Buffle, J., Leppard, G.G., 1995. Characterization of aquatic colloids and
629 macromolecules. 1. Structure and behavior of colloidal material. *Envir. Sci. Tech.*
630 29, 2169-2175.

631 Buffle, J., Wilkinson, K.J., Stoll, S., Filella, M., Zhang, J., 1998. A generalized
632 description of aquatic colloidal interactions: the three-colloidal component
633 approach. *Envir. Sci. Tech.* 32, 2887-2899.

634 Busenberg, E., Clemency, C.V., 1973. Determination of the cation exchange
635 capacity of clays and soils using an ammonia electrode. *Clay Clay Miner.* 21, 213-
636 217.

637 Citeau, L., Gaboriaud, F., Elsass, F., Thomas, F., Lamy, I., 2006. Investigation of
638 physico-chemical features of soil colloidal suspensions. *Colloid Surface A* 287,
639 94-105.

640 Clifton, J., Mcdonald, P., Plater, A., Oldfield, F., 1999. Investigation into the
641 efficiency of particle size separation using Stokes' Law. *Earth Surf. Proc. Land.*
642 24, 725-730.

643 Coppola, L., Gustafsson, Ö., Andersson, P., Eglinton, T.I., Uchida, M., Dickens,
644 A.F., 2007. The importance of ultrafine particles as a control on the distribution of
645 organic carbon in Washington Margin and Cascadia Basin sediments. *Chem.*
646 *Geol.* 243, 142-156.

647 De Lazzari, A., Rampazzo, G., Pavoni, B., 2004. Geochemistry of sediments in
648 the Northern and Central Adriatic Sea. *Estuar. Coast. Shelf S.* 59, 429-440.

649 Dolenc, T., Faganeli, J., Pirc, S., 1998. Major, minor and trace elements in
650 surficial sediments from the open Adriatic Sea: a regional geochemical study.
651 *Geol. Croat.* 51, 59-73.

652 Durn, G., Ottner, F., Slovenec, D., 1999. Mineralogical and geochemical
653 indicators of the polygenetic nature of terra rossa in Istria, Croatia. *Geoderma* 91,
654 125-150.

655 Durn, G., Rubinić, V., Wacha, L., Patekar, M., Frechen, M., Tsukamoto, S., Tadej,
656 N., Husnjak, S., 2018a. Polygenetic soil formation on Late Glacial Loess on the

657 Susak Island reflects paleo-environmental changes in the Northern Adriatic area.
658 *Quatern. Int.* 494, 236-247.

659 Durn, G., Wacha, L., Bartolin, M., Rolf, C., Frechen, M., Tsukamoto, S., Tadej, N.,
660 Husnjak, S., Li, Y., Rubinić, V., 2018b. Provenance and formation of the red
661 palaeosol and lithified terra rossa-like infillings on the Island of Susak: A high-
662 resolution and chronological approach. *Quatern. Int.* 494, 105-29.

663 Durn, G., Frechen, M., 2018c. Quaternary of Croatia. *Quatern. Int.* 494, 1-4.

664 Durn, G., Škapin, S.D., Vdović, N., Rennert, T., Ottner, F., Ružičić, S., Cukrov, N.,
665 Sondi, I., 2019. Impact of iron oxides and soil organic matter on the surface
666 physicochemical properties and aggregation of Terra Rossa and Calcocambisol
667 subsoil horizons from Istria. *Catena* 183, 104184.

668 Faganeli, J., Pezdič, J., Ogorelec, B., Mišič, M., Najdek, M., 1994. The origin of
669 sedimentary organic matter in the Adriatic. *Cont. Shelf Res.* 14, 365-384.

670 Gaffey, S.J., Bronnimann, C.E., 1993. Effects of bleaching on organic and mineral
671 phases in biogenic carbonates. *J. Sediment. Petrol.* 63, 752-754.

672 Giani, M., Djakovac, T., Degobbis, D., Cozzi, S., Solidoro, C., Fonda Umani, S.,
673 2012. Recent changes in the marine ecosystems of the northern Adriatic Sea.
674 *Estuar., Coast. Shelf S.* 115, 1-13.

675 Goudeau, M.L.S., Grauel, A.L., Bernasconi, S.M., de Lange, G.J., 2013.
676 Provenance of surface sediments along the southeastern Adriatic coast off Italy:
677 An overview. *Estuar. Coast. Shelf S.* 134, 45-56.

678 Gu, B., Schmitt, J., Chen, Z., Liang, L., McCarthy, J.F., 1994. Adsorption and
679 desorption of natural organic matter in iron oxide: mechanisms and models. *Envir.*
680 *Sci. Tech.* 28, 38-46.

681 Hardy, R., Tucker M., 1998. X-ray powder diffraction of sediments. In: Tucker, M.
682 (Ed.), *Techniques in Sedimentology*, Blackwell Scientific Publications, pp. 191-
683 228.

684 Hedges, J.I., Keil, R.G., 1995. Sedimentary organic matter preservation: an
685 assessment and speculative synthesis. *Mar. Chem.* 49, 81-115.

686 Hochella, M.F. Jr., Lower, S.K., Maurice, P.A., Lee Penn, R., Sahai, N., Sparks,
687 D.L., Twining, B.S., 2008. Nanominerals, mineral nanoparticles and Earth
688 systems. *Science* 319, 1631-1635.

689 Hunter, R. J., 1981. *Zeta Potential in Colloid Science*. Academic Press,
690 London/New York, pp. 386.

691 Ilijanić, N., Miko, S., Petrincec, B., Franić, Z., 2014. Metal deposition in deep
692 sediments from the Central and South Adriatic Sea. *Geol. Croat.* 67, 185-205.

693 Juračić, M., Prohić, E., 1991. Mineralogy, sources of particles, and sedimentation
694 in the Krka River estuary (Croatia). *Geološki Vjesnik* 44, 195-200.

695 Jurina, I., Ivanić, M., Vdović, N., Troškot-Čorbić, T., Lojen, S., Mikac, N., Sondi, I.,
696 2015. Deposition of trace metals in sediments of the deltaic plain and adjacent
697 coastal area (the Neretva River, Adriatic Sea). *J. Geochem. Explor.* 157, 120-131.

698 Kahle, M., Kleber, M., Torn, M.S., Jahn, R., 2003. Carbon storage in coarse and
699 fine clay fractions of illitic soils. *Soil Sci. Soc. Am. J.* 67, 1732-1739.

700 Kaiser, K., Eusterhues, K., Rumpel, C., Guggenberger, G., Kögel-Knabner, I.,
701 2002. Stabilization of organic matter by soil minerals - investigations of density
702 and particle-size fractions from two acid forest soils. *J. Plant Nutr. Soil Sc.* 165,
703 451-459.

704 Kaiser, K., Guggenberger, G., 2003. Mineral surfaces and soil organic matter.
705 *Eur. J. Soil Sci.* 54, 219-236.

706 Keil, R.G., Tsamakis, E., Fuh, C.B., Giddings, J.C., Hedges, J.I., 1994.
707 Mineralogical and textural controls on the organic composition of coastal marine
708 sediments: Hydrodynamic separation using SPLIT-fractionation. *Geochim.*
709 *Cosmochim. Ac.* 58, 879-893.

710 Keil, R.G., Tsamakis, E., Giddings, J.C., Hedges, J.I., 1998. Biochemical
711 distributions (amino acids, neutral sugars, and lignin phenols) among size-classes
712 of modern marine sediments from the Washington coast. *Geochim. Cosmochim.*
713 *Ac.* 62, 1347-1364.

714 Kleber, M., Mertz, C., Zikeli, S., Knicker, H., Jahn, R., 2004. Changes in surface
715 reactivity and organic matter composition of clay subfractions with duration of
716 fertilizer deprivation. *Eur. J. Soil Sci.* 55, 381–391.

717 Lojen, S., Sondi, I., Juračić, M., 2010. Geochemical conditions for the
718 preservation of recent aragonite-rich sediments in Mediterranean karstic marine
719 lakes (Mljet Island, Adriatic Sea, Croatia). *Mar. Freshwater Res.* 61, 119-128.

720 Matijević, S., Bogner, D., Morović, M., Tičina, V., Grbec, B., 2008. Characteristics
721 of the sediment along the eastern Adriatic coast (Croatia). *Fresen. Environ. Bull.*
722 17, 1763-1772.

723 Mayer, L.M., 1999. Extent of coverage of mineral surfaces by organic matter in
724 marine sediments. *Geochim. Cosmochim. Ac.* 63, 207-215.

725 Mikutta, R., Kleber, M., Kaiser, K., Jahn, R., 2005a. Review: organic matter
726 removal from soils using hydrogen peroxide, sodium hypochlorite, and disodium
727 peroxodisulfate. *Soil Sci. Soc. Am. J.* 69, 120-135.

728 Mikutta, R., Kleber, M., Jahn, R., 2005b. Poorly crystalline minerals protect
729 organic carbon in clay subfractions from acid subsoil horizons. *Geoderma* 128,
730 106-115.

731 Moore, D.M., Reynolds, R.C., 1989. X-ray Diffraction and the Identification and
732 Analysis of Clay Minerals. Oxford University Press, Oxford, pp. 378.

733 Morse, J.W., Arvidson, R.S, Lüttge, A., 2007. Calcium carbonate formation and
734 dissolution. *Chem. Rev.* 107, 342-381.

735 Perret, D., Newman, M.E., Nègre, J.C., Chen, Y., Buffle, J., 1994. Submicron
736 particles in the Rhine river - I. physico-chemical characterization. *Water Res.* 28,
737 91-106.

738 Pigorini, B., 1968. Sources and dispersion of recent sediments of the Adriatic
739 Sea. *Mar. Geol.* 6, 187-229.

740 Pikelj, K., Juračić, M., 2013. Eastern Adriatic Coast (EAC): geomorphology and
741 coastal vulnerability of a karstic coast. *J. Coastal Res.* 29(4), 944-957.

742 Pikelj, K. Jakšić, L., Aščić, Š., Juračić, M., 2016. Characterization of the fine-
743 grained fraction in the surface sediment of the eastern Adriatic channel areas.
744 *Acta Adriat.* 57(2), 195-208.

745 Plathe, K.L., von der Kammer, F., Hassellöv, M., Moore, J.N., Murayama, M.,
746 Hofmann, T., Hochella, M.F.Jr., 2013. The role of nanominerals and mineral
747 nanoparticles in the transport of toxic trace metals: Field-flow fractionation and
748 analytical TEM analyses after nanoparticle isolation and density separation.
749 *Geochim. Cosmochim. Ac.* 102, 213-225.

750 Range, K.J., Range, A., Weiss, A., 1969. Fire-clay type kaolinite or fire-clay
751 mineral? Experimental classification of kaolinite–halloysite minerals. *Proceedings*
752 *of the 3rd International Clay Conference*, Tokyo 1, 3-13.

753 Ransom, B., Kim, D., Kastner, M., Wainwright, S., 1998. Organic matter
754 preservation on continental slopes: importance of mineralogy and surface area.
755 *Geochim. Cosmochim. Ac.* 62, 1329-1345.

756 Ravaioli, M., Alvisi, F., Menegazzo Vitturi, L., 2003. Dolomite as a tracer for
757 sediment transport and deposition on the northwestern Adriatic continental shelf
758 (Adriatic Sea, Italy). *Cont. Shelf Res.* 23, 1359-1377.

759 Rivaro, P., Ianni, C., Massolo, S., Ruggieri, N., Frache, R., 2004. Heavy metals in
760 Albanian coastal sediments. *Toxicol. Environ. Chem.* 86, 85-97.

761 Rodriguez-Navarro, C. Di Lorenzo, F., Elert, K., 2018. Mineralogy and
762 physicochemical features of Saharan dust wet deposited in the Iberian Peninsula
763 during an extreme red rain event. *Atmos. Chem. Phys.* 18, 10089-10122.

764 Shepard, F.P., 1954. Nomenclature based on sand-silty-clay ratios. *J. Sediment*
765 *Petrol.* 24, 151-154.

766 Sondi, I., Milat, O., Pravdić, V., 1997. Electrokinetic potentials of clay surfaces
767 modified by polymers. *J. Colloid Interf. Sci.* 189, 66-73.

768 Sondi, I., Juračić, M., 2010. Whiting events and the formation of aragonite in
769 Mediterranean karstic marine lakes: new evidence on its biologically induced
770 inorganic origin. *Sedimentology* 57, 85-95.

771 Sondi, I., Mikac, N., Vdović, N., Ivanić, M., Furdek, M., Škapin, S., 2017.
772 Geochemistry of recent aragonite-rich sediments in Mediterranean karstic marine
773 lakes: Trace elements as pollution and palaeoredox proxies and indicators of
774 authigenic mineral formation. *Chemosphere* 168, 786-797.

775 Spagnoli, F., Dinelli, E., Giordano, P., Marcaccio, M., Zaffagnini, F., Frascari, F.,
776 2014. Sedimentological, biogeochemical and mineralogical facies of Northern and
777 Central Western Adriatic Sea. *J. Marine Syst.* 139, 183-203.

778 Tang, Z., Wu, L., Luo, Y., Christie, P., 2009. Size fractionation and
779 characterization of nanocolloidal particles in soils. *Environ. Geochem. Hlth.* 31, 1-
780 10.

781 Tomadin, L., 2000a. Sedimentary fluxes and different dispersion mechanisms of
782 the clay sediments in the Adriatic Basin. *Rend. Lincei-Sci Fis.* 9/11, 161-174.

783 Tomadin, L., 2000b. Riverborne and wind-blown kaolinite in the present clay
784 sediments of the Adriatic Sea. *Acta Universitatis Carolinae, Geologica* 44, 2-4,
785 157-161.

786 Tombacz, E., Szekeres, M., 2004. Colloidal behavior of aqueous montmorillonite
787 suspensions: the specific role of pH in the presence of indifferent electrolytes.
788 *Appl. Clay Sci.* 27, 75-94.

789 Toševski, A., Grgec, D., Padovan, B., 2012. Some characteristics of Eocene
790 flysch genesis, composition and weathering in Croatian coast belt. *The Mining-
791 Geology-Petroleum Engineering Bulletin* 25, 47-62 (in Croatian).

792 Vdović, N., Bišćan, J., Juračić, M., 1991. Relationship between specific surface
793 area and some chemical and physical properties of particulates: study in the
794 northern Adriatic. *Mar. Chem.* 36, 317-328.

795 Vdović, N., Juračić, M., 1993. Sedimentological and surface characteristics of the
796 northern and central Adriatic sediments. *Geol. Croat.* 46/1, 157-163.

797 Wentworth, C.K., 1922. A scale of grade and class terms for clastic sediments. *J.
798 Geol.* 30, 377-392.

799 Wilkin, R.T., Barnes, H.L., Brantley, S.L., 1996. The size distribution of framboidal
800 pyrite in modern sediments: an indicator of redox conditions. *Geochim.
801 Cosmochim. Ac.* 60, 3897-3912.

802 Wilkinson, K.J., Reinhardt, A., 2005. Contrasting roles of organic matter on
803 colloidal stabilization and flocculation in freshwaters. In: Droppo, I.G., Leppard,
804 G.G., Liss, S.N., Milligan, T.G. (Eds.), *Flocculation in Natural and Engineered
805 Environmental Systems*, CRC Press, pp. 147-170.

806 Zhuang, J., Yu, G.R., 2002. Effects of surface coatings on electrochemical
807 properties and contaminant sorption of clay minerals. *Chemosphere* 49, 619-628.

Table 1. Mineral composition of the investigated native sediments, the OM removal efficiency and the TOC content before (native) and after the NaOCl treatment (treated_{NaOCl}).

Sample	TOC, mass. %	OM removal efficiency %	carbonates mass. %	Mineral composition of the native sediment samples	
	<i>Native / treated_{NaOCl}</i>			major constituents	minor constituents
S1	0.47 / 0.17	64	27	Quartz, Phyllosilicates	Feldspars, Calcite, Dolomite, Pyrite
S2	0.92 / 0.16	82	59	Calcite, Quartz, Pyrite	Phyllosilicates
S3	0.51 / 0.09	82	28	Calcite, Phyllosilicates	Mg-Calcite, Quartz, Feldspars
S4	0.35 / 0.17	53	37	Calcite, Phyllosilicates	Mg-Calcite, Quartz, Feldspars,
S5	0.63 / 0.11	82	30	Calcite, Dolomite, Quartz, Phyllosilicates	Feldspars, Pyrite
S6	1.52 / 0.30	81	69	Aragonite, Mg-Calcite, Pyrite	Calcite, Quartz, Phyllosilicates, Feldspars
S7	0.88 / 0.18	80	15	Phyllosilicates, Quartz, Feldspars	Calcite
S8	0.43 / 0.20	54	14	Quartz, Phyllosilicates	Feldspars, Calcite

Table 2. Mineral composition of the separated size fractions of the investigated

Sample	Size fraction (µm)	Mean size (µm)	Calcite	Mg-calcite	Aragonite	Dolomite	Quartz	Plagioclase	K-feldspar	Pyrite	Illite	Chlorite	Smectite	KI _D	KI	MLCM	I/S MLCM
S1	<2	0.4	+				+	+	+	+	XXX	X	X	X	X		XX
	<1	0.3	+				+			+	XX		X		X		XXX
S2	<2	0.4	+				+			+	XX			X	XX		XX
	<1	0.2	+				+			+	XX				XX		XX
S3	<2	0.4	+				+	+			XXX	XX	XX	X	X	X	
	<1	0.2	+				+				XXX	XX	XXX		X	X	
S5	<2	0.4	+			+	+	+		+	XXX	XX	X	X	X	X	X
	<1	0.2	+			+	+			+	XXX	X	XX	X	X	X	X
S6	<2	0.5	+	+	+		+	+	+	+	XX			X	XX	X	
	<1	0.2	+	+	+		+			+	XX				XX		
S7	<2	0.4	+				+	+			XXX	X	X		?	X	
	<1	0.2	+				+				XXX	X	X		?	X	
	<0.45	0.1	+				+				XXX	X	X		?	X	
S8	<1	0.2	+				+				XXX	X	XX		?	X	XX
	<0.45	0.1	+				+				XX	X	XXX		?	X	X

“+” non-clay mineral present in the sample

“X” relative abundance of clay minerals based on X-ray diffraction (no quantitative value is assigned to X)

“KI_D” Kaolinite that forms intercalation compounds with DMSO

“KI” Kaolinite that does not intercalate with DMSO

“MLCM” mixed-layer clay minerals in which type of interstratification and constituting clay minerals were not recognized with certainty

“I/S MLCM” Illite-smectite mixed-layer clay mineral

“?” mineral phase was not detected with certainty

sediments.

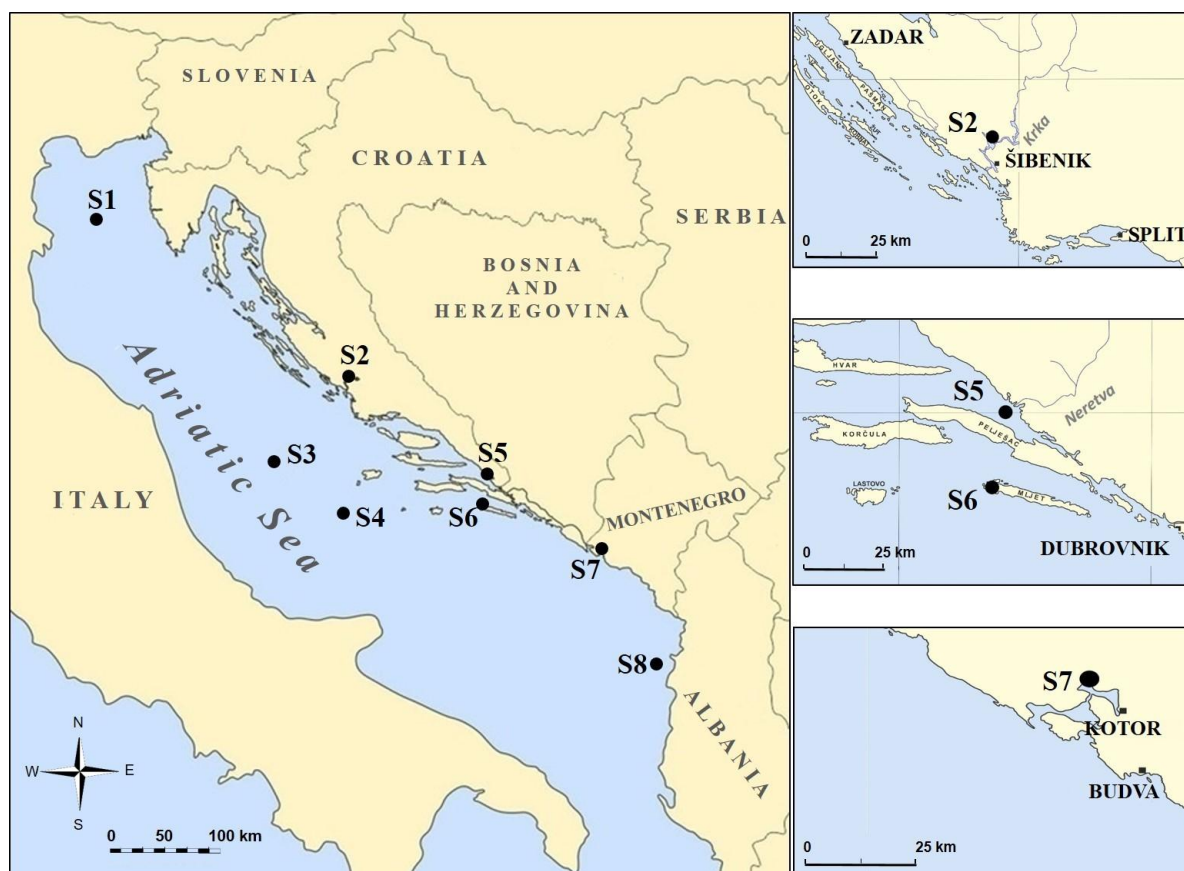


Figure 1. Map of the investigated area with sampling stations and their depth: S1 – northern Adriatic (36 m); S2 - Krka River estuary (6 m); S3 - central Adriatic open-sea (266 m); S4 - central Adriatic open-sea (166 m); S5 - Neretva Channel (30 m); S6 - Malo Jezero, island of Mljet (28 m); S7 - Risan Bay (33 m); S8 – open-sea in front of Albanian coast (100 m).

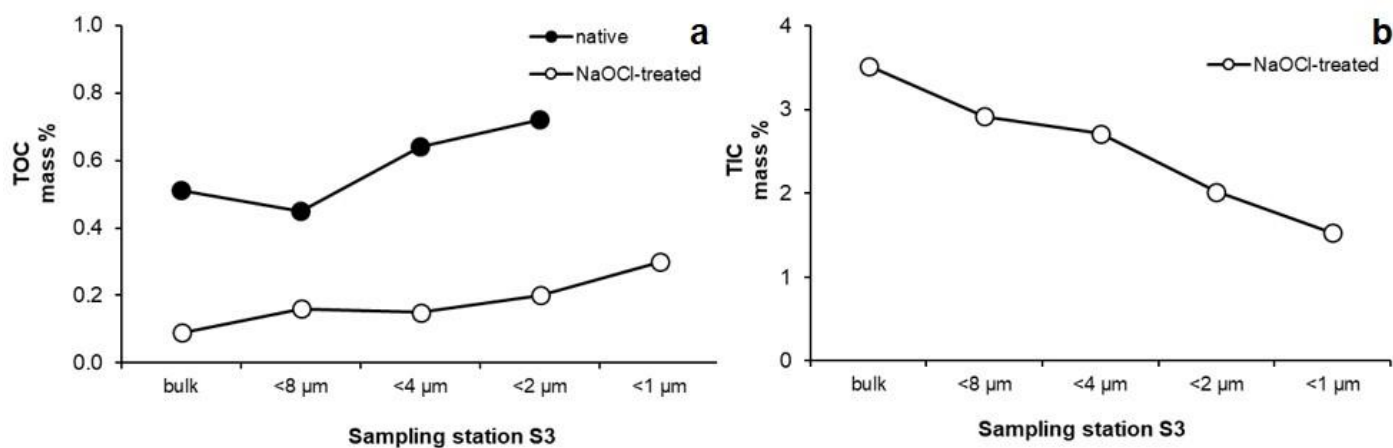


Figure 2. Size fractions separated from the sampling station S3 showing: (a) the TOC content in the native and the NaOCl-treated size fractions and (b) the TIC content in the NaOCl-treated size fractions.

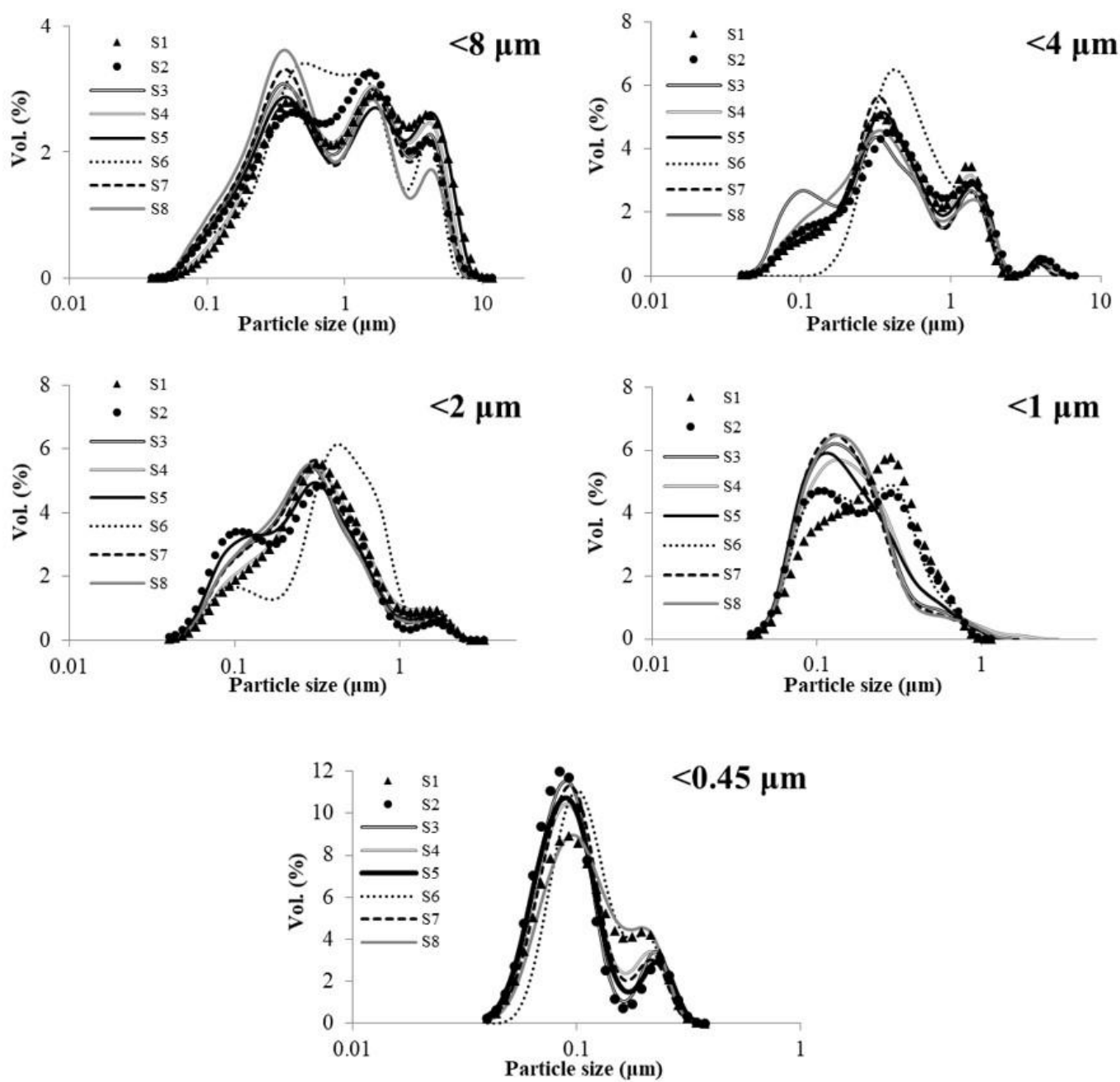


Figure 3. PSD curves of fractions (<8 μm, <4 μm, <2 μm, <1 μm, <0.45 μm) separated from the NaOCl-treated sediment samples.

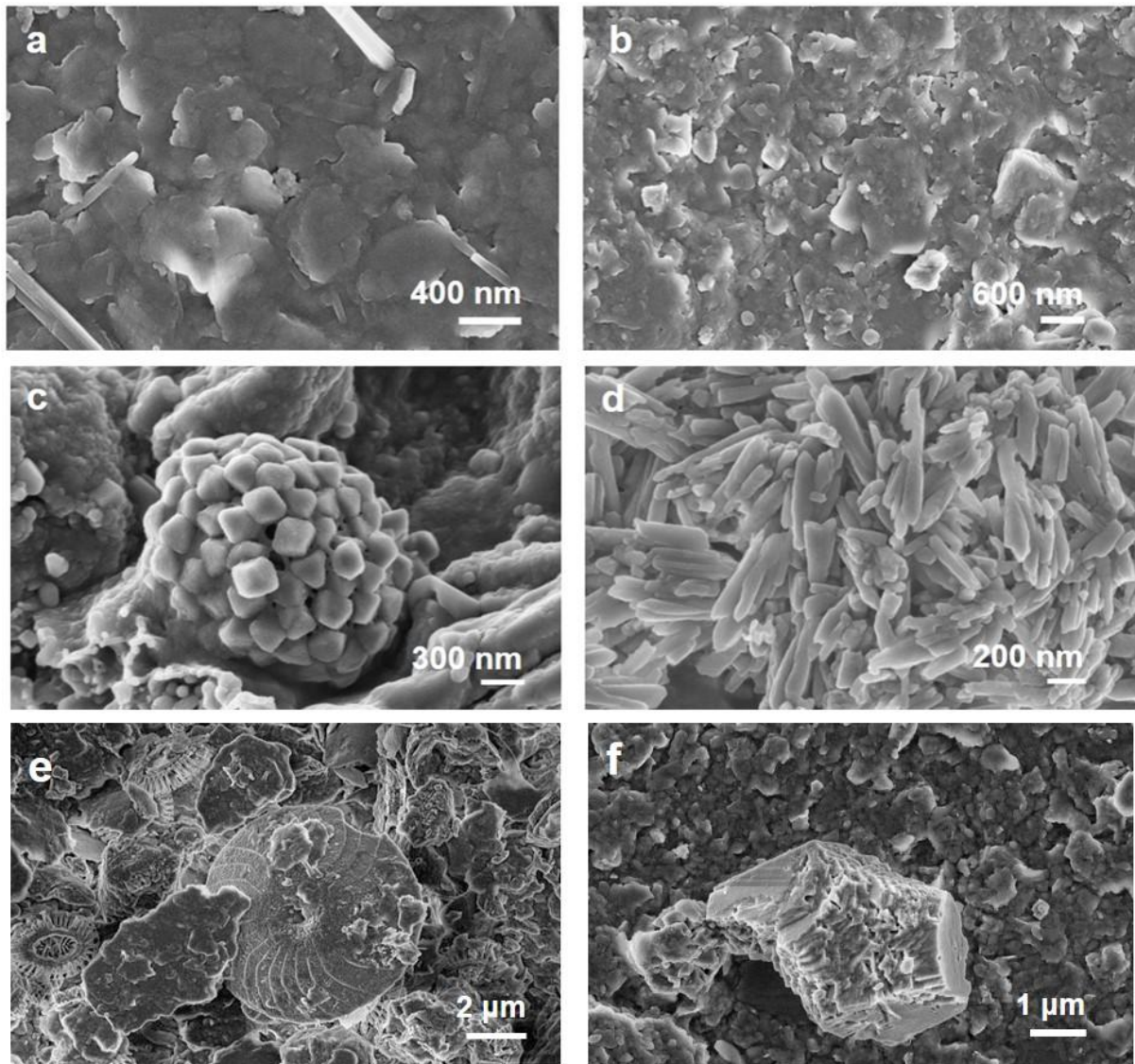


Figure 4. FE-SEM photomicrographs showing: (a) phyllosilicates in sediment from the Albanian coastal area (S8) and (b) in sediment of the Risan Bay (S7); (c) diagenetic framboidal pyrite and (d) inorganically precipitated aragonite in sediment from Malo Jezero on the island of Mljet (S6); (e) prevalence of biogenic detritus in

sediment from the central Adriatic open-sea area (S3); (f) calcite in dominantly phyllosilicate submicrometer fraction from the Krka River estuary (S2).

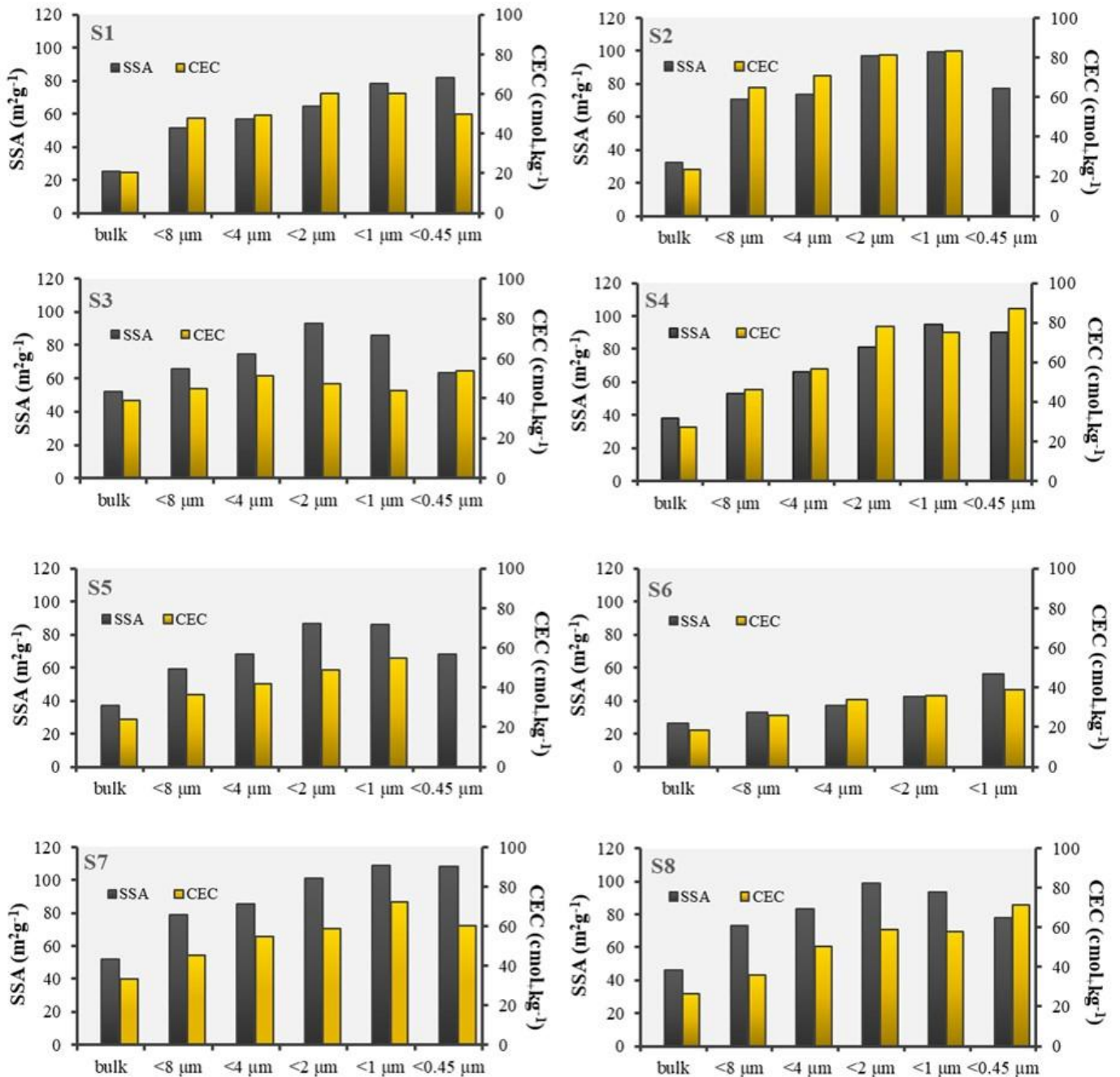
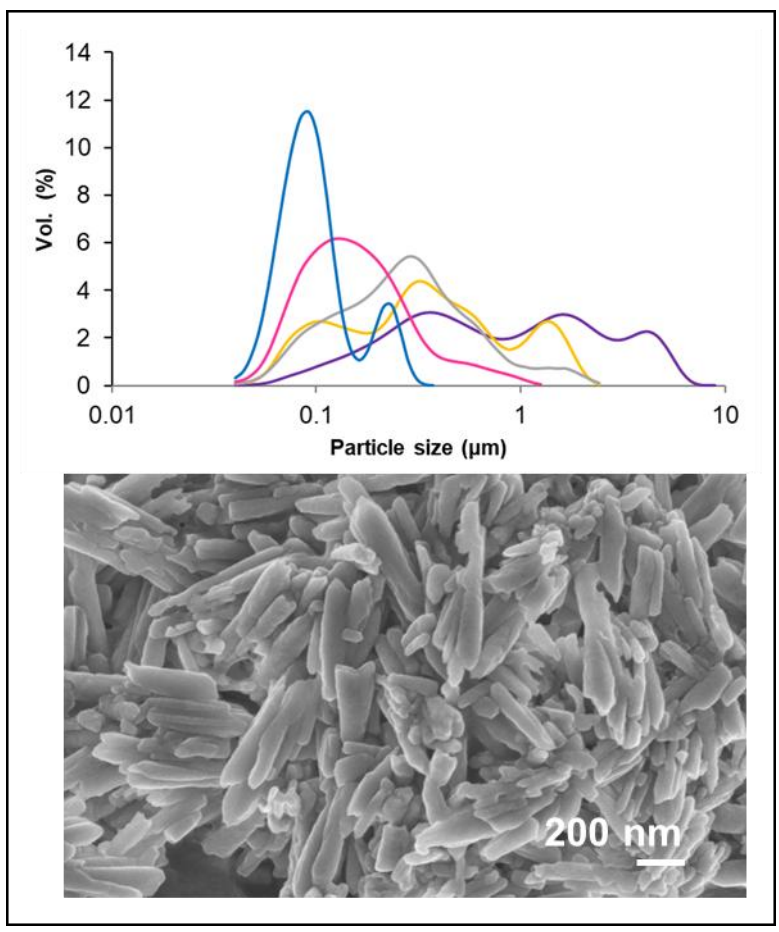


Figure 5. SSA and CEC of different size fractions of sediments after the OM removal.

Supplementary Material

[Click here to download Supplementary Material: Supplementary.docx](#)



Declaration of interests

The authors declare that they have no known competing financial interests or personal relationships that could have appeared to influence the work reported in this paper.

The authors declare the following financial interests/personal relationships which may be considered as potential competing interests: